Supplementary Materials

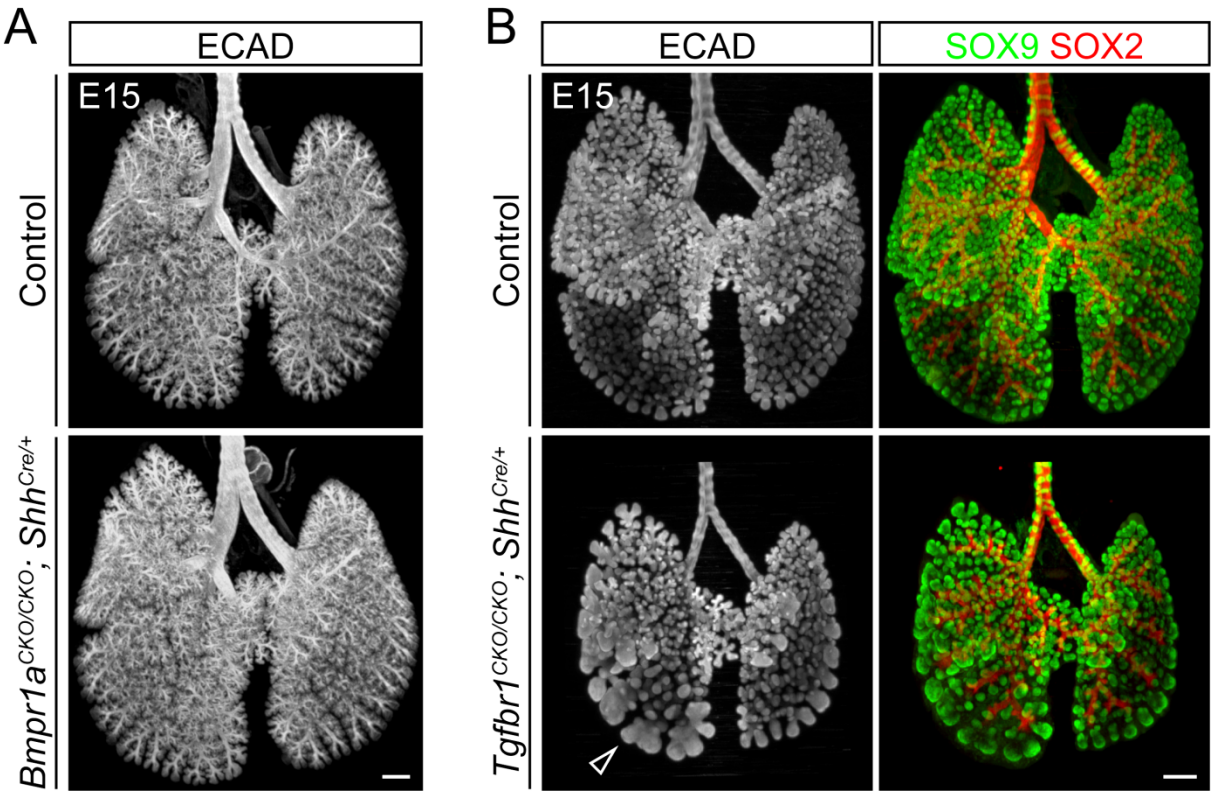

Figure S1. Epithelial *Bmpr1a* and *Tgfbr1* mutant lungs.

(A) OPT projection images showing normal lung morphology of the *Bmpr1a*$^{CKO/CKO}$; *Shh*$^{Cre/+}$ mutant in comparison to the littermate control lung. Scale: 250 um. At least 3 lungs for each genotype have been examined with consistent results.

(B) OPT projection images of immunstained *Tgfrb1*$^{CKO/CKO}$; *Shh*$^{Cre/+}$ mutant and littermate control lungs. The *Tgfrb1* mutant lung is smaller with dilated branch tips (open arrowhead) but normal distribution of SOX9 and SOX2 staining. Scale: 250 um. At least 3 lungs for each genotype have been examined with consistent results.

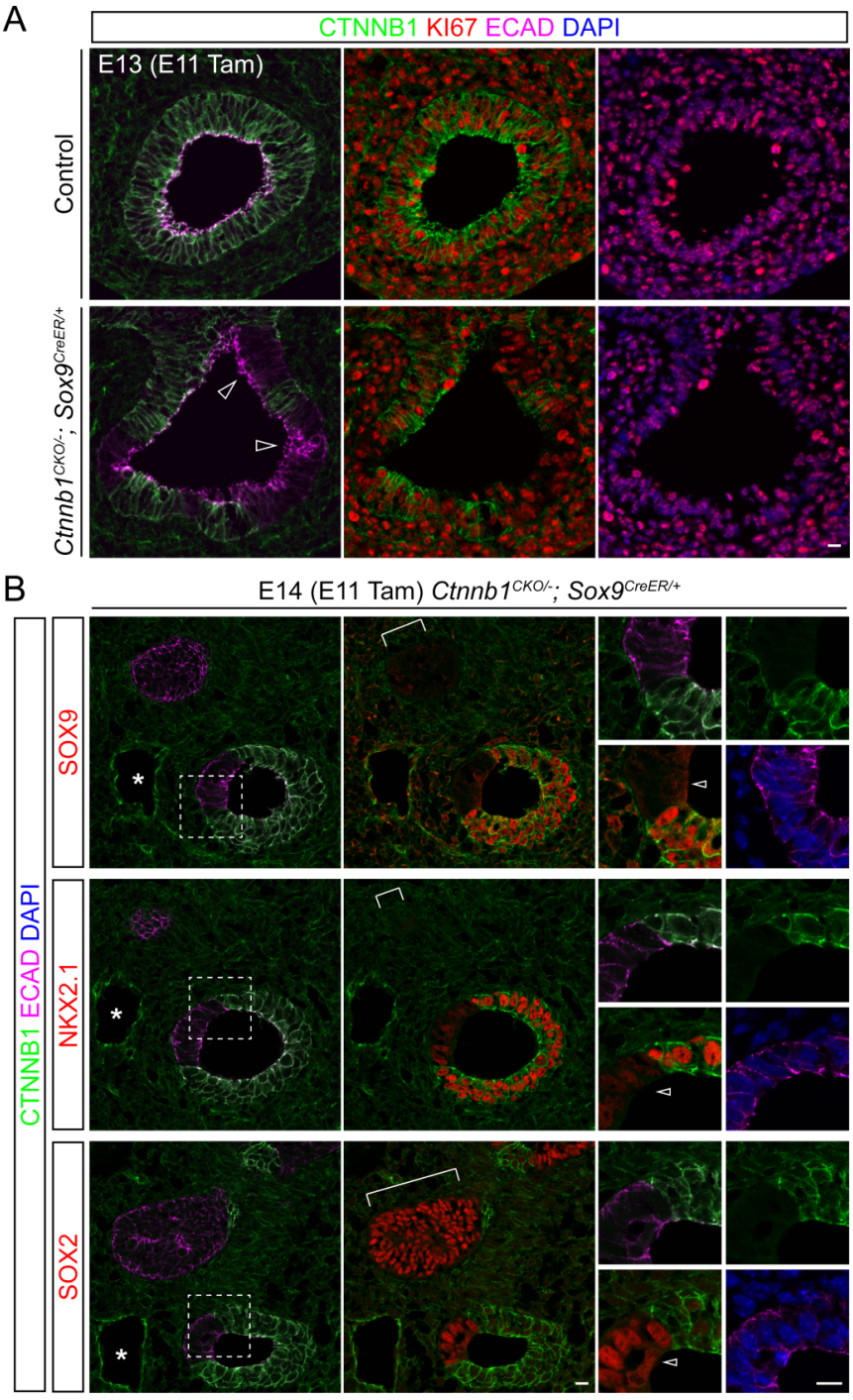

Figure S2. *Ctnnb1* mutant cells are proliferative and SOX9 loss, NKX2.1 downregulation, and ectopic SOX2 expression are concurrent.

(A) Confocal images of immunostained lung sections from E13 *Ctnnb1*$^{CKO/-}$; *Sox9*$^{CreER/+}$ mutant and littermate control embryos with Cre recombination induced at E11 with 2 mg of tamoxifen (Tam). The epithelium is marked by ECAD and also identifiable by its compact cell arrangement. *Ctnnb1* mutant cells (open arrowheads) express a proliferative marker Ki67. Scale: 10 um. At least 3 sections for each lung and at least 3 lungs for each genotype have been examined with consistent results.

(B) Confocal images of immunostained consecutive sections from E14 *Ctnnb1*$^{CKO/-}$; *Sox9*$^{CreER/+}$ mutant and littermate control lungs with Cre recombination induced by 1 mg of tamoxifen (Tam) at E11. The epithelium is marked by ECAD and also identifiable by its compact cell arrangement. Asterisks indicate the same vessel on the consecutive sections. Boxed regions are enlarged to show the sharp boundaries between control and *Ctnnb1* mutant (open arrowheads) cells. Square brackets indicate additional examples. Scale: 10 um.

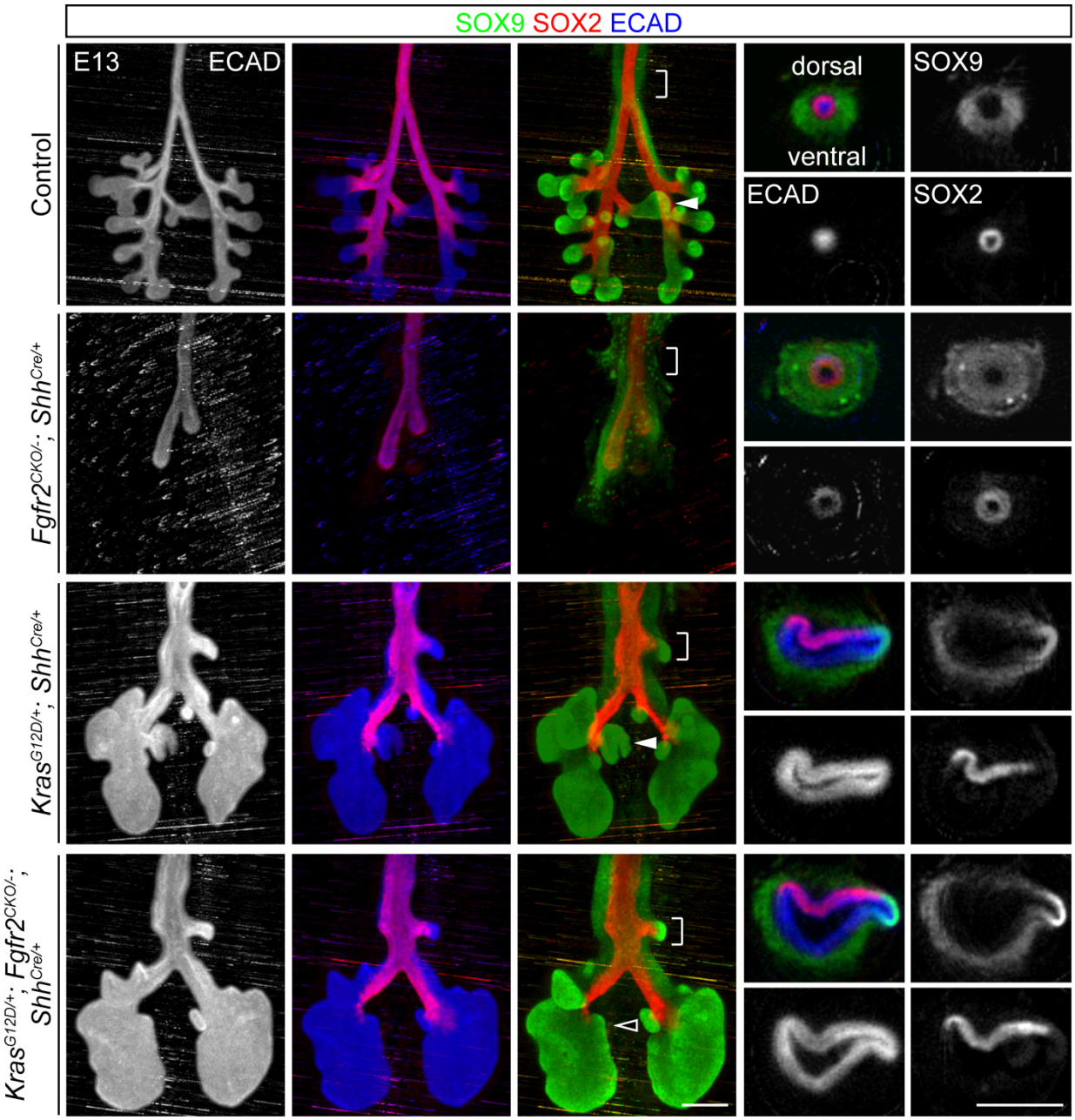

Figure S3. The *Kras* gain-of-function mutation is genetically epistatic to the *Fgfr2* loss-of-function mutation using *Shh*^{Cre}.

OPT projection and section images of whole-mount immunostained E13 lungs of indicated genotypes. The *Kras*/*Fgfr2* double mutant recapitulates the *Kras* single mutant phenotypes including overgrown branches and ectopic tracheal branches (optical sections at the level indicated by square brackets) with the exception of improper lobation pattern including the absence of the accessory lobe (compare open versus filled arrowheads). Scale: 250 um. At least 2 lungs for each genotype have been examined with consistent results.

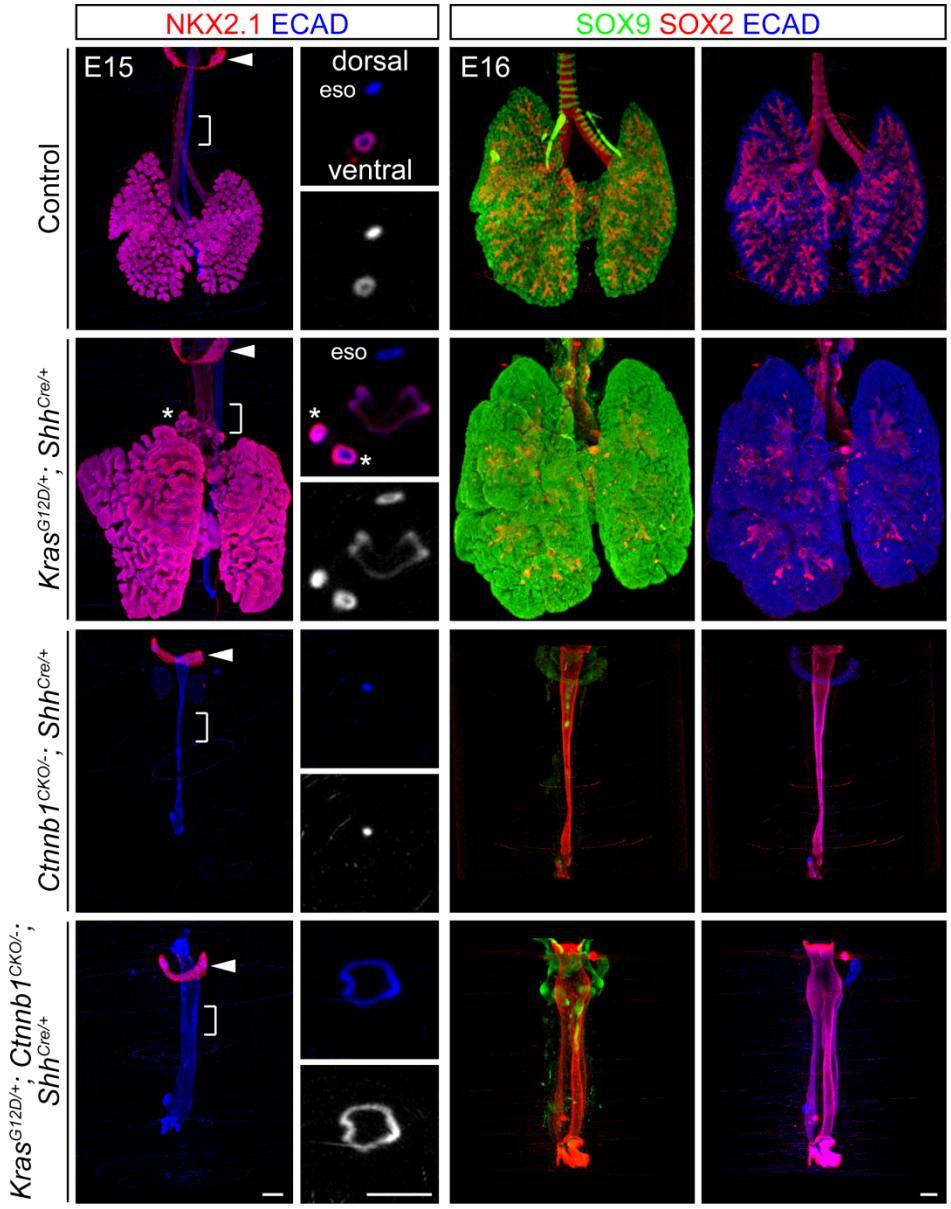

Figure S4. The *Ctnnb1* loss-of-function mutation is genetically epistatic to the *Kras* gain-of-function mutation using *Shh*^{Cre}.

OPT projection and section images of whole-mount immunostained E15 and E16 lungs of indicated genotypes. The *Ctnnb1*/*Kras* double mutant recapitulates the *Ctnnb1* single mutant phenotypes including failure to form NKX2.1-expessing lung cells and to separate the esophagus (eso) and the trachea (optical sections at the level indicated by square brackets) with the exception of a dilated fused trachea/esophagus tube. The phenotype is specific to the lung since NKX2.1 expression is normal in the thyroids (filled arrowheads). Asterisks indicate ectopic tracheal branches in the *Kras* single mutant, a phenotype also suppressed by the *Ctnnb1* mutation. Scale: 250 um. At least 2 lungs for each genotype have been examined with consistent results.

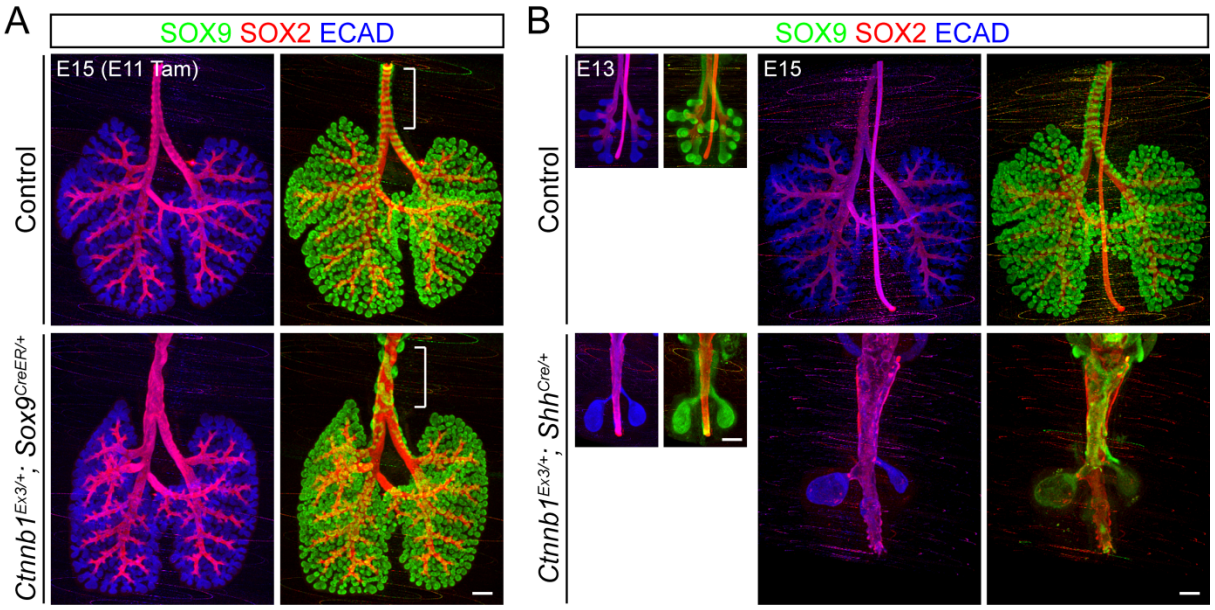

Figure S5. Genetic stabilization of CTNNB1 by *Sox9*^{CreER} does not affect SOX9 progenitors.

(A) OPT projection images of whole-mount immunostained E15 *Ctnnb1*$^{Ex3/+}$*; Sox9*$^{CreER/+}$ mutant and littermate control lungs with Cre recombination induced by 3.5 mg of tamoxifen (Tam) at E11. Although cartilage rings, which are also targeted by *Sox9*^{CreER}, are disrupted (square brackets), branching and SOX9/SOX2 expression are normal. Scale: 250 um. At least 3 lungs for each genotype have been examined with consistent results.

(B) OPT projection images of whole-mount immunostained E13 and E15 *Ctnnb1*$^{Ex3/+}$*; Shh*$^{Cre/+}$ mutant and littermate control lungs. Unlike (A), CTNNB1 stabilization before lung specification blocks branching and trachea-esophagus separation. SOX9 expression diminishes after E13 perhaps secondary to the blockage in branching and associated pathways. Scale: 250 um. At least 2 lungs for each genotype have been examined with consistent results.

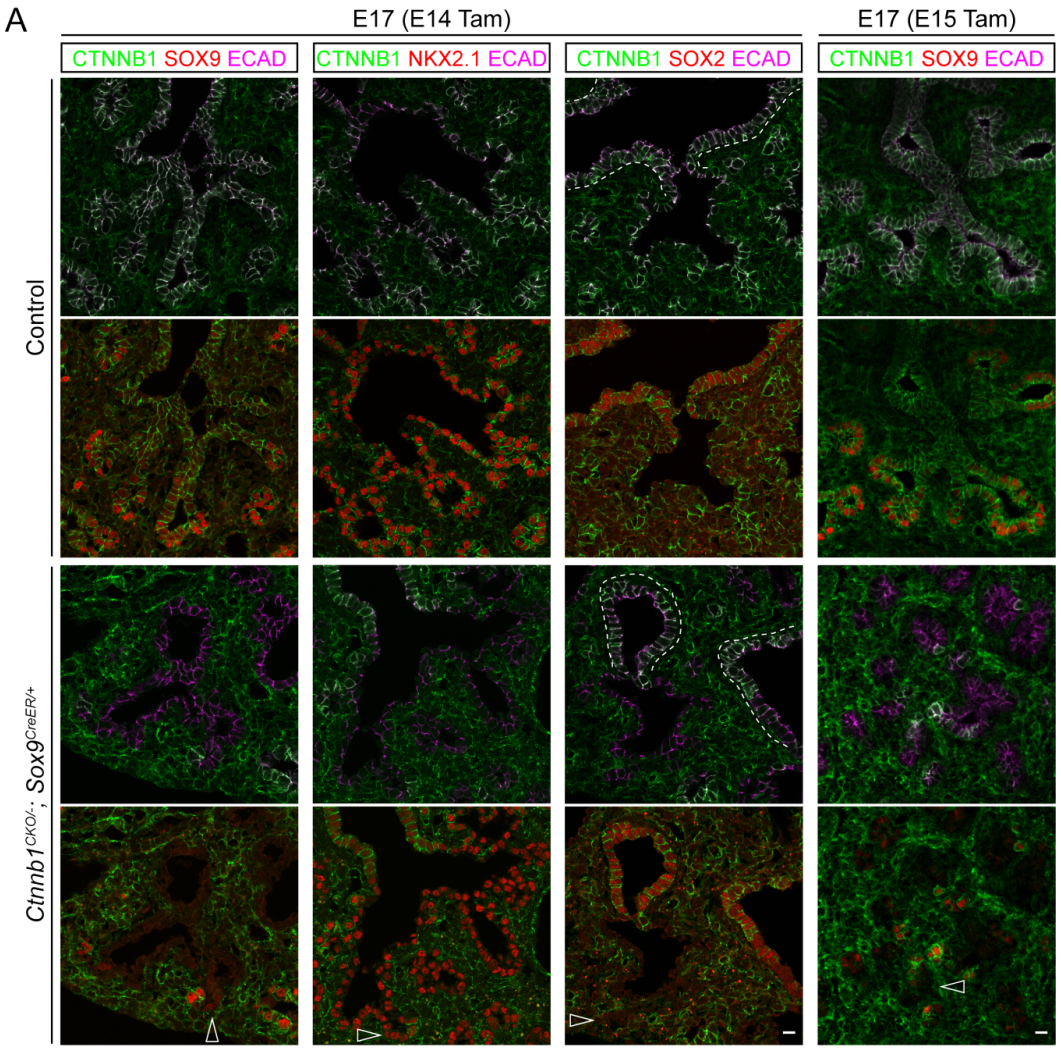

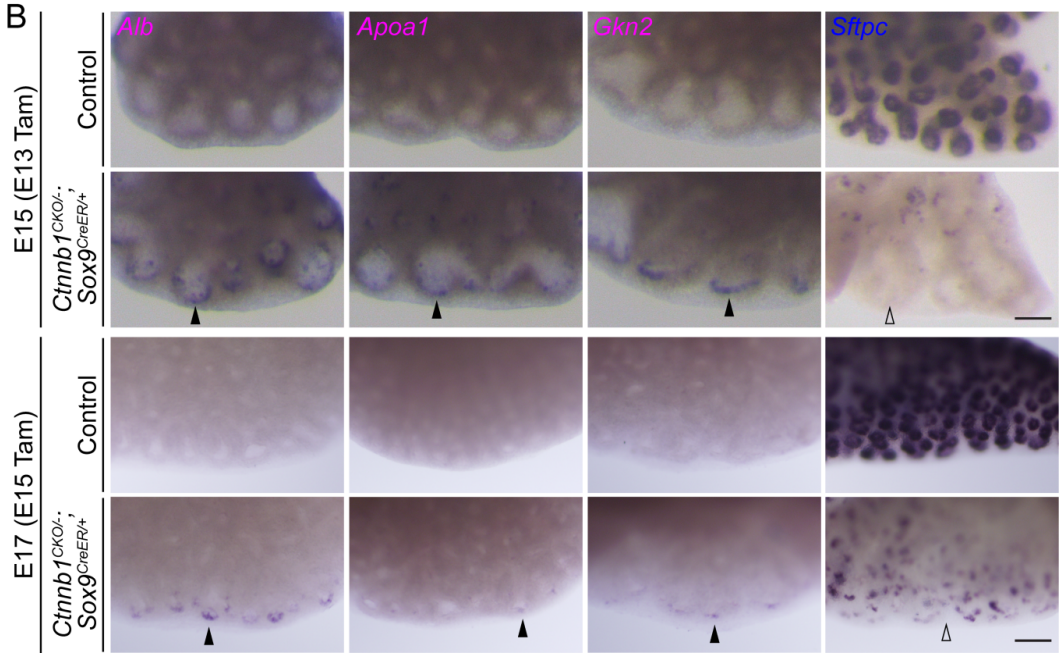

Figure S6. *Ctnnb1* deletion at E14 leads to cell-autonomous loss of SOX9 with no change in NKX2.1 and SOX2.

(A) Confocal images of immunostained lung sections from E17 *Ctnnb1*$^{CKO/-}$; *Sox9*$^{CreER/+}$ mutant and littermate control embryos with Cre recombination induced by 2 mg of tamoxifen (Tam) at E14 (left three columns) or E15 (rightmost column). *Ctnnb1* mutant cells (open arrowheads; magenta ECAD but no green CTNNB1 staining) cell-autonomously lose SOX9, but have normal NKX2.1 and SOX2 expression. Dashes indicate conducting airways, which are identified by the compact ECAD staining but have a lower level of SOX2 expression compared to lungs at earlier developmental stages due to variability in fixation of older lungs. Scale: 10 um. At least 3 sections for each lung and at least 2 lungs for each genotype have been examined with consistent results.

(B) Whole-mount in situ hybridization of E15 (top) or E17 (bottom) *Ctnnb1*$^{CKO/-}$; *Sox9*$^{CreER/+}$ mutant and littermate control lungs with Cre recombination induced by 3.5 mg of tamoxifen (Tam) at E13 or E15, respectively. GI genes are derepressed (filled arrowheads) in fewer mutant progenitors when recombination is induced at E15 albeit with comparable loss of *Sftpc* (open arrowheads). Whole-mount, instead of section, images are used to visualize the infrequent cells expressing the GI genes. The *Sftpc* images of the E15 lungs are duplicated from Fig. 6A for comparison with the E17 lungs. Scale: 100 um. At least 2 lungs for each genotype have been examined with consistent results.

A

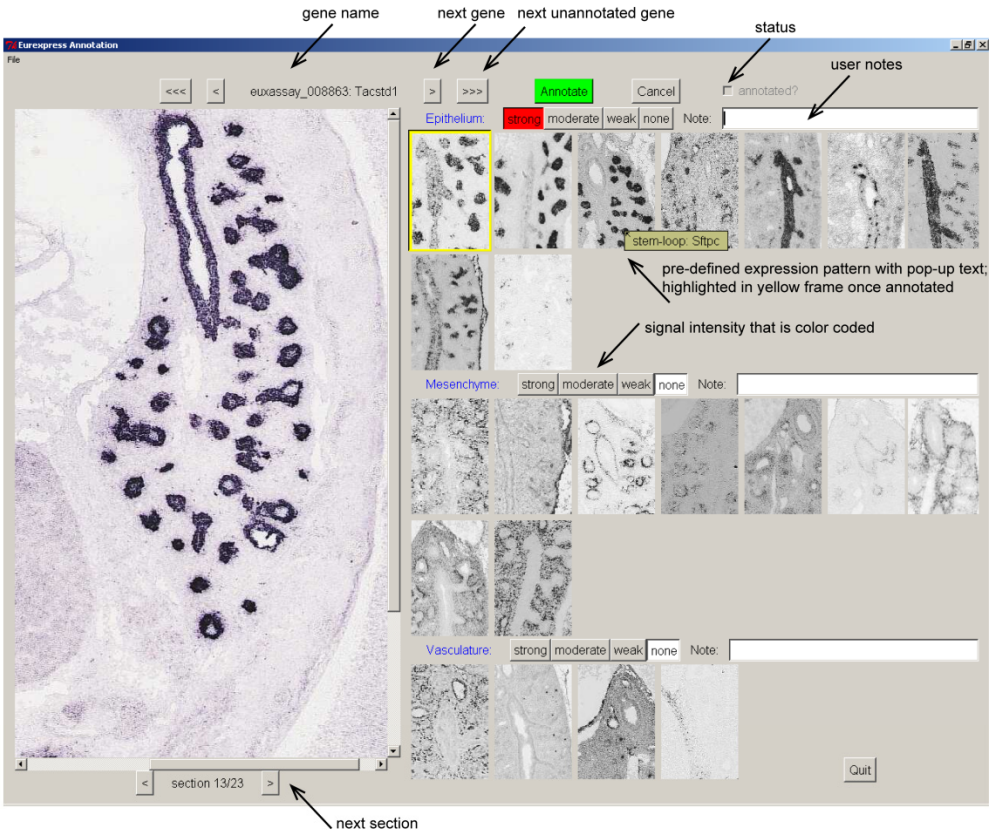

B

compartment	code	expression pattern	example gene
epithelium	A	all epithelium and uniform	Nkx2-1
	B	all epithelium, but higher distally	Irx1
	C	distal epithelium, tip and stalk	Sftpc
	D	distal epithelium, tip	Id2
	E	proximal epithelium	Sox2
	F	sporadic proximal epithelium	Ascl1
	G	proximal epithelium with a lower level distally	Anxa1
	H	stalk enriched	Smoc2
	I	sporadic distal epithelium	Dctn4
mesenchyme	A	all mesenchyme and uniform	Tbx4
	B	methothelium	Wt1
	C	subepithelial mesenchyme	Tgfbi
	D	distal stalk subepithelial mesenchyme	Ptch1
	E	distal tip subepithelial mesenchyme	Stip1
	F	smooth muscle	Psd
	G	submethothelial mesenchyme	Fgf10
	H	smooth muscle around stalks	Gypc
	I	all mesenchyme but at a higher level near epithelium	Pdgfrb
vasculature and others	A	all vessels	Pecam1
	B	sporadic: neurons or leukocytes	Gata1
	C	artery smooth muscle	Ankrd1
	D	diaphram	Lgi1
	E	mature vessels	Fbln5

Figure S7. Eurexpress screen user interface.

(A) User interface of a custom PERL (practical extraction and report language) code that downloads in situ images of specific sections and genes from Eurexpress and allows users to annotate them by selecting from predefined expression patterns.

(B) Predefined expression patterns with their alphabetical codes and example genes.

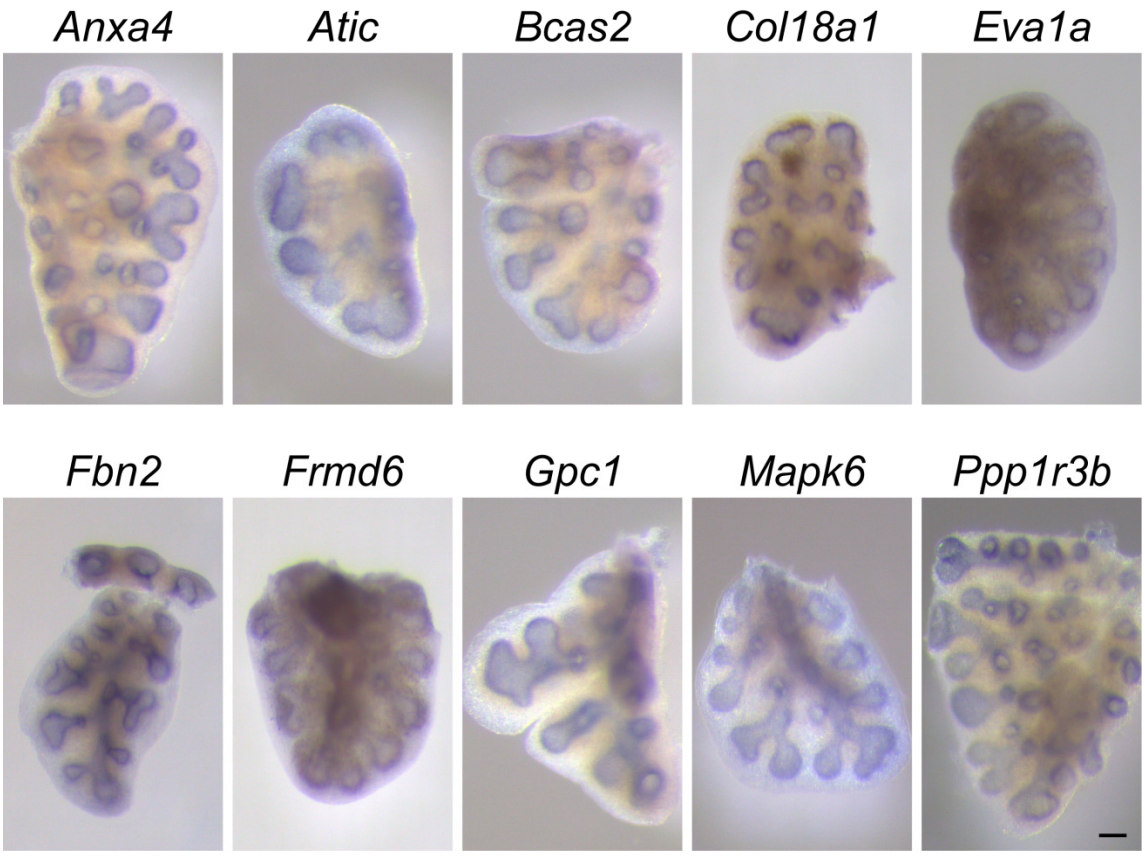

Figure S8. Confirmation of a subset of new progenitor genes from the Eurexpress screen.

Whole-mount in situ hybridization of indicated genes on E13 or E14 lung lobes. Scale: 100 um.

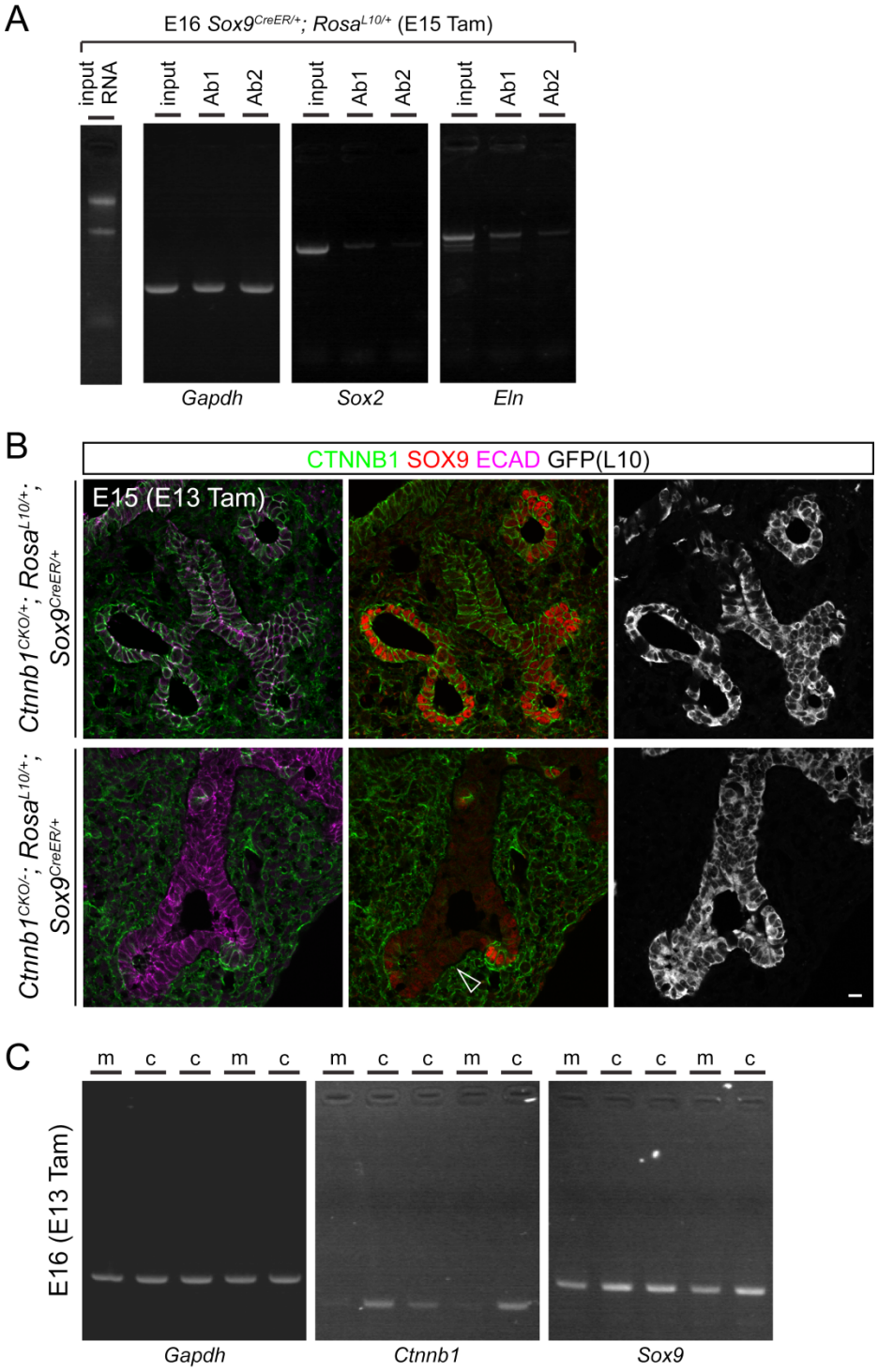

Figure S9. *Sox9*^{CreER} TRAP-RNAseq method.

(A) TRAP using two independent GFP antibodies (Ab1 and Ab2) of E16 *Sox9*$^{CreER/+}$; *Rosa*$^{L10/+}$ lungs with Cre recombination induced by 2 mg of tamoxifen (Tam) at E15. The input is kept on ice for the duration of the TRAP immunoprecipitation, verifying that RNA remains intact under the experimental conditions. RT-PCR shows depletion of a proximal epithelial marker (*Sox2*) and a mesenchymal marker (*Elastin*, *Eln*). See Fig. 5A for enrichment of progenitor genes.

(B) Confocal images of immunostained sections from E15 mutant (*Ctnnb1*$^{CKO/-}$; *Rosa*$^{L10/+}$; *Sox9*$^{CreER/+}$) and littermate control (*Ctnnb1*$^{CKO/+}$; *Rosa*$^{L10/+}$; *Sox9*$^{CreER/+}$) lungs with Cre recombination induced by 3.5 mg of tamoxifen (Tam) at E13. The epithelium is marked by ECAD and also identifiable by its compact cell arrangement. The *Rosa*^{L10} allele recombines more readily than the *Ctnnb1*^{CKO} allele, although most epithelial cells lose CTNNB1 and SOX9 in the mutant lung with a high dosage of tamoxifen (open arrowhead). Scale: 10 um. At least 3 sections for each lung and at least 2 lungs for each genotype have been examined with consistent results.

(C) RT-PCR analyses of TRAP RNAs from E16 mutant (m, *Ctnnb1*$^{CKO/-}$; *Rosa*$^{L10/+}$; *Sox9*$^{CreER/+}$) and littermate control (c, *Ctnnb1*$^{CKO/+}$; *Rosa*$^{L10/+}$; *Sox9*$^{CreER/+}$) lungs with Cre recombination induced by 3.5 mg of tamoxifen (Tam) at E13. Note downregulation of *Ctnnb1* in the mutants with unaffected mesenchymal expression (see (B)), indicating successful purification of the epithelial RNAs by TRAP. *Sox9* downregulation is modest possibly due to the semi-quantitative nature of the PCR assay, but is better quantified by RNAseq in Fig. 5B.

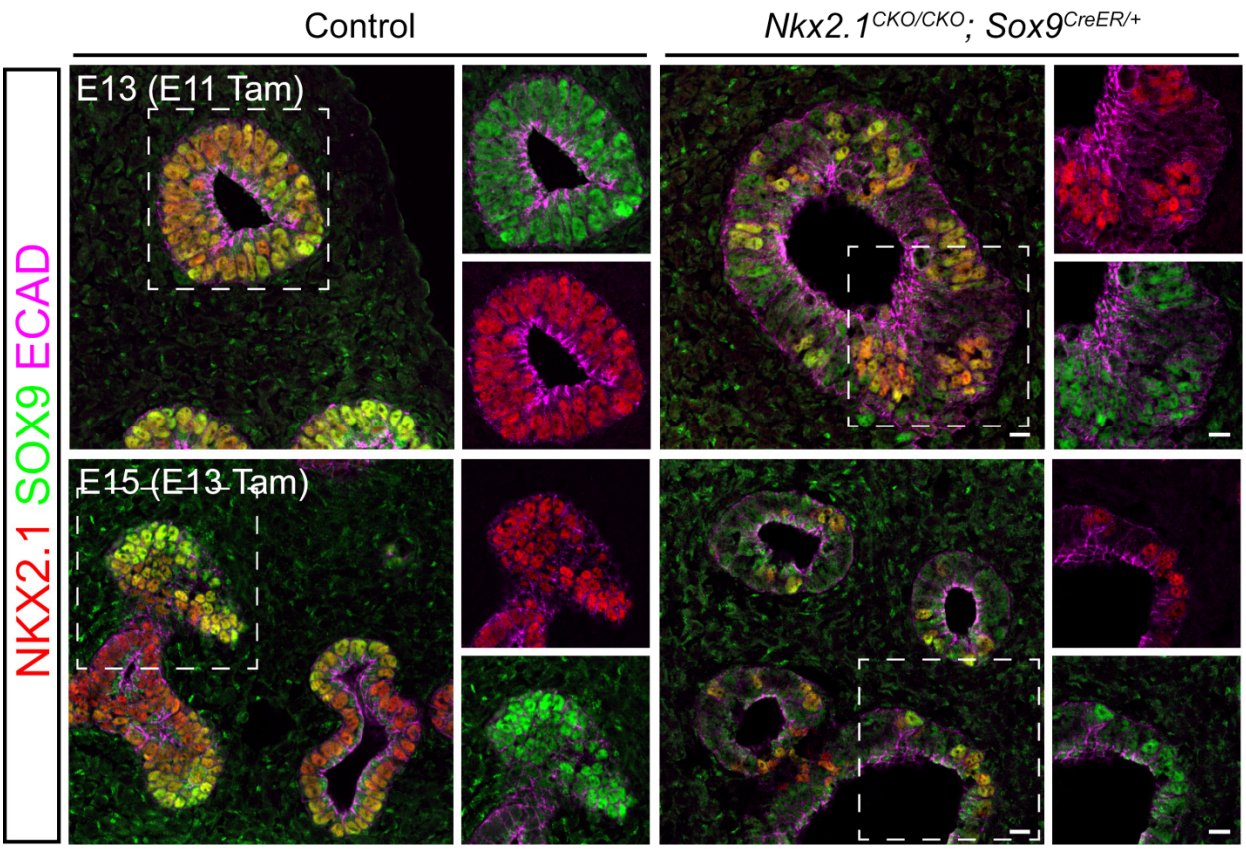

Figure S10. *Nkx2.1* deletion leads to loss of SOX9.

Confocal images of immunostained sections from E13 (top) or E15 (bottom) *Nkx2.1*$^{CKO/CKO}$; *Sox9*$^{CreER/+}$ mutant and littermate control lungs with Cre recombination induced with 2 mg tamoxifen (Tam) at E11 or E13, respectively. The epithelium is marked by ECAD and also identifiable by its compact cell arrangement. Boxed regions are enlarged. Mosaic deletion of *Nkx2.1* leads to cell-autonomous loss of SOX9. Scale: 10 um. At least 3 sections for each lung have been examined with consistent results.

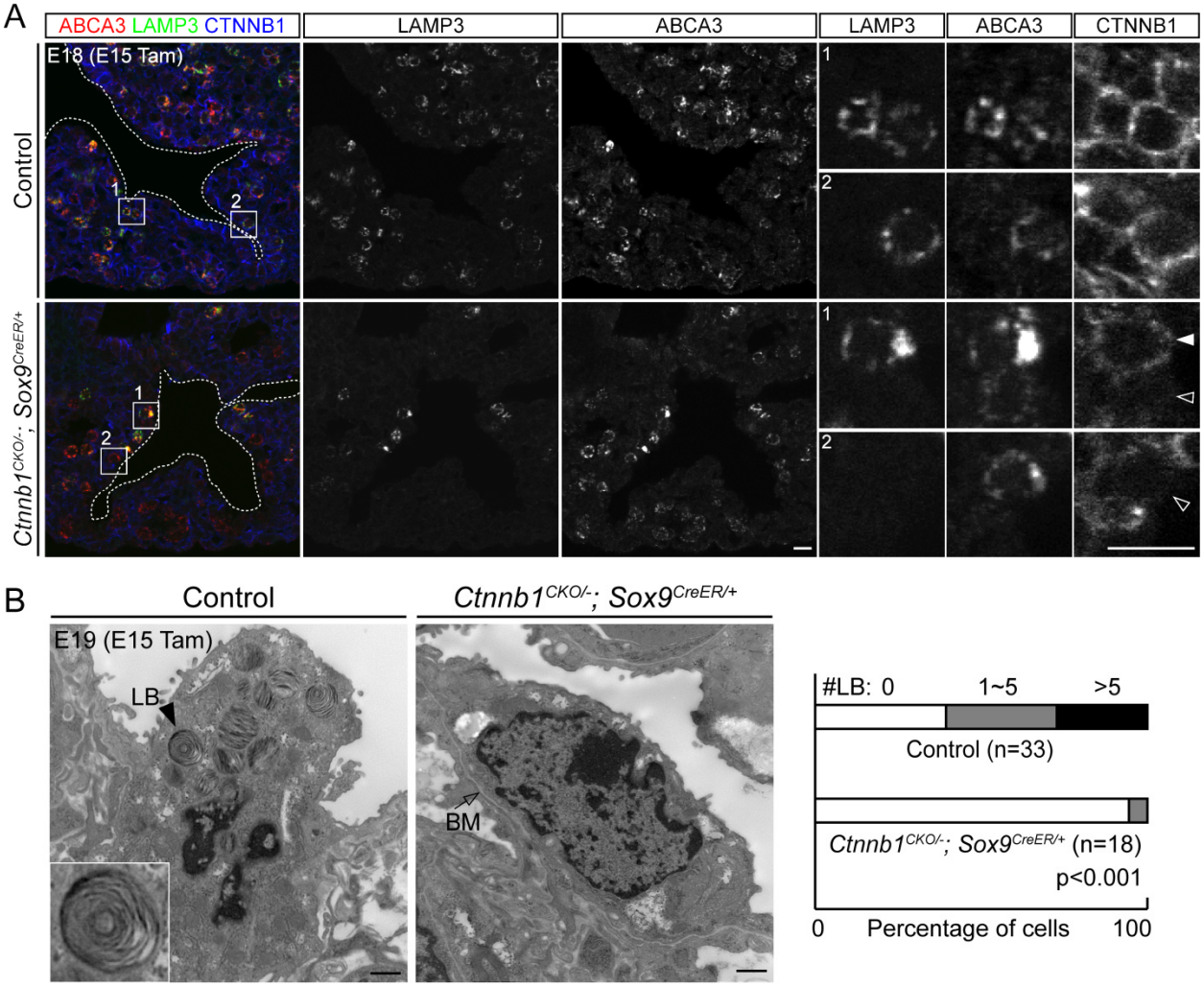

Figure S11. *Ctnnb1* deletion disrupts alveolar differentiation.

(A) Confocal images of immunostained sections from E18 *Ctnnb1*$^{CKO/-}$*; Sox9*$^{CreER/+}$ mutant and littermate control lungs with Cre recombination induced by 3.5 mg of tamoxifen (Tam) at E15. The epithelial lumen is outlined with dashes. The mutant lung has fewer LAMP3 cells but comparable ABCA3 staining; the remaining LAMP3 staining can be attributed to unrecombined epithelial cells. At E18, the lung has started alveolar differentiation, making it challenging to distinguish epithelial versus mesenchymal CTNNB1 staining. Numbered boxed regions are enlarged to show that LAMP3 and ABCA3 expressing cells in the control lung are surrounded by cuboidal CTNNB1 staining, but that in the mutant lung some ABCA3 expressing cells are no longer surrounded by cuboidal CTNNB1 staining nor express LAMP3 (open arrowheads), which is in contrast to adjacent unrecombined control cells (filled arrowhead). Note CTNNB1 is unaffected in surrounding mesenchymal cells. Scale: 10 um. At least 3 sections for each lung and at least 2 lungs for each genotype have been examined with consistent results.

(B) Transmission electron microscopy images from E19 *Ctnnb1*$^{CKO/-}$*; Sox9*$^{CreER/+}$ mutant and littermate control lungs with Cre recombination induced by 3.5 mg of tamoxifen (Tam) at E15. LB, lamellar body; BM, basement membrane. The number of lamellar bodies in cuboidal cells that are above the basement membrane is quantified, showing defects in lamellar body formation in the *Ctnnb1* mutant lung (p=0.0004, Fisher's exact test). Scale: 1 um.

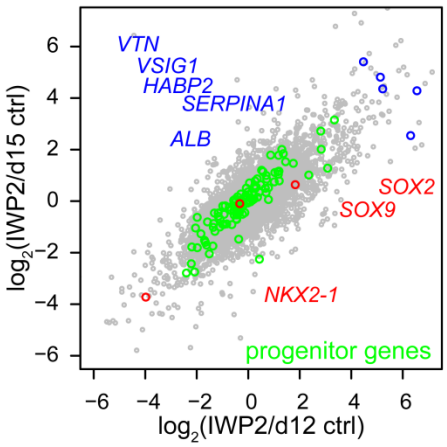

Figure S12. Further inhibition of endogenous WNT production by IWP2 led to comparable changes in *NKX2.1*, GI genes, and *SOX9*-like progenitor genes

REUS2 cells were cultured according to the protocol in Figure 7A. Scatterplot of log 2 fold change in RNAseq FPKM values comparing d15 with a WNT production inhibitor IWP2 versus d12 control (ctrl; x-axis) or d15 control (y-axis). Gene names are approximately aligned horizontally to the corresponding color-coded data points to avoid interference with the scatterplot. Blue: GI genes according to annotations by the Human Protein Atlas (www.proteinatlas.org). Green: the human orthologs of the mouse progenitor genes, which are not consistently downregulated in comparison to the *Ctnnb1* mutant mouse lung (Fig. 5B). Only genes with an average FPKM value greater than 1 are plotted.

Table S1. Eurexpress screen results.

List of genes with a high signal-to-noise ratio (level=3) in Eurexpress images. Note that some genes have more than one expression patterns. Symbol X and level 0 indicate no discernible expression. Refer to Fig. S7B for the alphabetic code of the expression pattern.

Click here to Download Table S1

Table S2. List of 119 progenitor genes.

Click here to Download Table S2

Table S3. FPKM values of *Sox9*^{CreER} TRAP-RNAseq of control lungs for Fig. 5A.

Click here to Download Table S3

Table S4. FPKM values of *Sox9*^{CreER} TRAP-RNAseq of *Ctnnb1* mutant and littermate control lungs for Fig. 5B.

Click here to Download Table S4

Table S5. FPKM values of RNAseq of cultured human lung progenitor for Fig. 7B and S12.

Click here to Download Table S5

Table S6. FPKM values of progenitor genes in mice and human cells from Table S3, S4, and S5.

Click here to Download Table S6